Chemistry & Biology
Article

Insights into Protein-Protein and Enzyme-Substrate Interactions in Modular Polyketide Synthases

Lucky Tran,[1] R. William Broadhurst,[1,*] Manuela Tosin,[1,2] Andrea Cavalli,[2] and Kira J. Weissman[3,*]
[1]Department of Biochemistry, 80 Tennis Court Road, University of Cambridge, Cambridge CB2 1GA, UK
[2]Department of Chemistry, Lensfield Road, University of Cambridge, Cambridge CB2 1GE, UK
[3]Pharmaceutical Biotechnology, Saarland University, P.O. Box 151150, 66041 Saarbrücken, Germany
*Correspondence: r.w.broadhurst@bioc.cam.ac.uk (R.W.B.), k.weissman@mx.uni-saarland.de (K.J.W.)
DOI 10.1016/j.chembiol.2010.05.017

SUMMARY

Numerous natural products of clinical value are biosynthesized by polyketide synthases (PKSs) and nonribosomal peptide synthetases (NRPSs), which are multienzymes comprising modules of catalytic domains. The key players in each module are carrier proteins, which serve as attachment points for the growing substrate chains. Thus, the details of carrier protein-based substrate delivery to each active site are central to understanding chain assembly in these systems. In the enterobactin NRPS, communication between a peptidyl carrier protein (PCP) and the adjacent thioesterase (TE) domain occurs through formation of a compact complex. Using NMR, we show that the corresponding interaction between a PKS acyl carrier protein (ACP) and its downstream TE is fundamentally different: chain transfer occurs in the absence of a protein-protein interface, with contact limited to the substrate acyl terminus.

INTRODUCTION

The polyketides are a structurally diverse class of natural products, with applications in human and veterinary medicine. Biosynthesis of these metabolites in bacteria is accomplished by enzymatic machineries with highly divergent architectures. Aromatic polyketides are typically generated by type II polyketide synthases (PKSs), iteratively acting multienzyme complexes comprising a small set of discrete proteins. In contrast, in the construction of reduced polyketides, the biosynthetic tasks are performed by protein domains housed within gigantic multienzymes (type I PKS) (Staunton and Weissman, 2001; Fischbach and Walsh, 2006). In the modular class of type I PKS, the domains are organized into functional units called "modules," such that each module accomplishes a single round of chain extension. The central component of each module is a small (~10 kDa), noncatalytic acyl carrier protein (ACP) domain, to which the growing intermediates are tethered in covalent linkage to a phosphopantetheine (Ppant) cofactor. Posttranslational attachment of Ppant is carried out in *trans* by a dedicated phosphopantetheinyl transferase (PPTase) (Lambalot et al., 1996). Analysis of a typical chain extension cycle reveals that the ACP must communicate with all other domains within the module to either receive or present substrate (Figure 1A). Faithful polyketide assembly also requires that these ACP-based interactions are regulated, so that the ACP cooperates with all catalytic partners within its module, before transfer of the growing chain to the subsequent module (Weissman and Müller, 2008).

The assembly line logic of PKS systems is also found in nonribosomal peptide synthetases (NRPSs), modular multienzymes that condense a programmed series of amino acids into small peptide metabolites. In NRPS systems, chain extension intermediates are tethered to peptidyl carrier protein (PCP) domains, which share the core structural fold of ACP domains (Alekseyev et al., 2007; Weber et al., 2000). Frueh et al. recently solved the solution structure of an *apo* PCP (a PCP lacking its Ppant prosthetic group) from the enterobactin NRPS, attached to its natural downstream partner, the chain-releasing thioesterase (TE) (Frueh et al., 2008). The two domains form a tight complex, in which the active sites are juxtaposed at a suitable distance for substrate transfer. Similarly, the PCP has a specific binding contact with the adjacent chain-extending condensation (C) domain. Based on NMR studies of a PCP from the tyrocidine (Tyc) NRPS, dynamic modulation of the structure is suggested to guide selection of the appropriate partner domain within the chain extension modules (Koglin et al., 2006). In its *apo* form, the Tyc PCP domain occupies two stable conformations (called the A and A/H states). Conversion to the *holo* form by addition of Ppant, however, shifts the A-state equilibrium to the alternative H-state equilibrium, comprising the A/H and H states. The A state is preferentially recognized by the PPTase, and the H state by an externally operating, proof-reading thioesterase (TEII) domain (Yeh et al., 2004; Schwarzer et al., 2002). Although such conformational selection has so far only been demonstrated for these *trans*-acting enzymes, the data support a model in which conformational variability of the PCP is also used to program alternative protein-protein interactions with potential partners within the multienzymes.

Given the similarities between PKS and NRPS systems, it has been suggested that partner choice in modular PKSs may also be guided by conformational switching (Frueh et al., 2008; Weissman and Müller, 2008; Kapur and Khosla, 2008; Lai et al., 2006). High-resolution structural information is currently available for only a single type I PKS ACP domain, ACP_2 from the erythromycin (DEBS) PKS, in its *apo* form (Alekseyev et al., 2007). The domain was not reported to exhibit any conformational variation. Structures have also been determined by NMR and X-ray crystallography for many ACP domains derived from

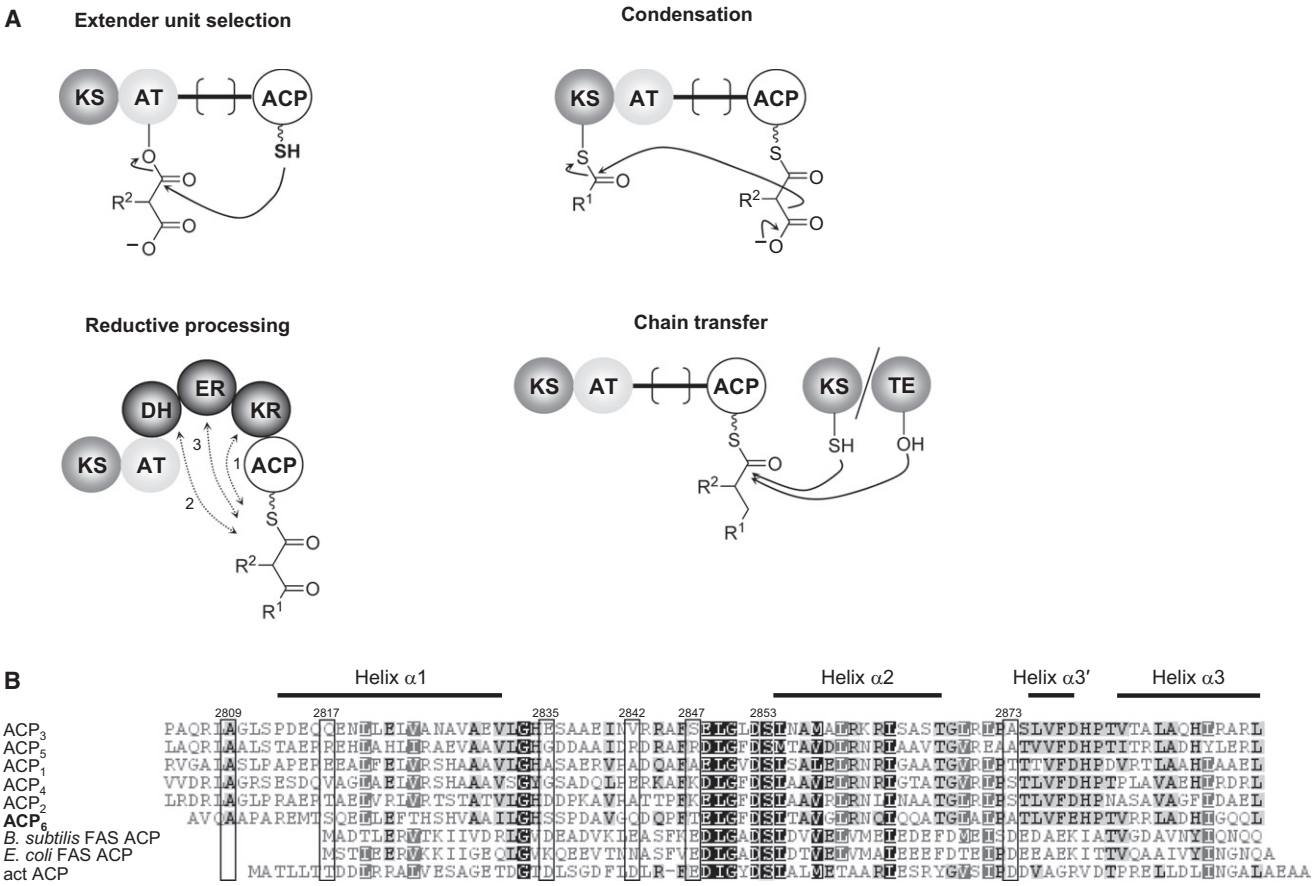

Figure 1. ACP Analysis

(A) Consideration of a typical round of chain extension shows that the acyl-ACP domain must interact with all of the catalytic domains housed within the PKS module: with the AT to receive the extender unit, with the KS to participate in the Claisen-like condensation, and with any reductive domains which are present. Subsequently, it engages in chain transfer with a domain located in a downstream module, a KS or a TE.

(B) Multiple sequence alignment (ClustalW) of the ACP domains from the DEBS system (ACPs 1–6), with those from the actinorhodin type II PKS (act ACP), and the type II FAS ACPs of *Bacillus subtilis* and *Escherichia coli*. Residue numbering is according to the EryAIII protein (NCBI reference sequence YP_001102991.1). Residues mentioned in the text are highlighted. The secondary structural elements as determined for ACP_2 are shown (Alekseyev et al., 2007).

type II PKS in their *apo*, *holo*, and acyl-modified forms (Evans et al., 2008; Findlow et al., 2003; Li et al., 2003), as well as for ACPs of the type II fatty acid synthases (FASs) (Kim et al., 2006; Zornetzer et al., 2006; Xu et al., 2001; Roujeinikova et al., 2002; Wong et al., 2002); despite sharing low overall sequence homology with type I ACPs (as low as 4% identity) (Figure 1B), all of the ACP domains exhibit a similar α-helical fold (Alekseyev et al., 2007). Although both *apo* and *holo* type II ACPs (Kim et al., 2006; Li et al., 2003; Findlow et al., 2003; Zornetzer et al., 2006) show some conformational heterogeneity, many *holo* proteins do not interact stably with their appended Ppant arms (Wong et al., 2002; Xu et al., 2001; Kim et al., 2006; Li et al., 2003). In these cases, the *apo* and *holo* forms of the domains are essentially identical, and therefore the Ppant-induced conformational modulation observed for NRPS PCPs does not appear to be a conserved feature of PKS and FAS ACP domains. In addition, recent work by us (Tran et al., 2008) and others (Chen et al., 2007) has challenged the underlying assumption that ACP domains in type I PKS systems must always form a protein-protein complex in order to interact with partner domains. For example, PKS ketoreductase (KR) domains exhibit a high degree of tolerance toward multiple ACP partners, suggesting that the KR domains instead recognize ACP-tethered acyl chains (Chen et al., 2007).

Here, we report that another type I ACP, ACP_6 from the DEBS PKS, adopts a single conformation in solution in both its *apo* and *holo* forms, as judged by solution phase NMR. Furthermore, as we find no evidence that the domain interacts substantially with its Ppant cofactor, we conclude that the *apo* and *holo* forms are effectively equivalent. No contacts were observed to any of several acyl chains when they were tethered in thioester linkage to the ACP, further arguing against the conformational switching model. Although transfer of the model substrate butyrate from the ACP to the adjacent TE is highly efficient (Tran et al., 2008), transacylation occurs in the absence of a defined protein-protein interface between the ACP and TE domains; instead recognition by the TE may be limited to the C1 carbonyl group of the substrate acyl chain. Taken together, these data show that effective communication between acyl-ACP and TE occurs solely as a result of the covalent tethering of the domains within a single multienzyme (Tran et al., 2008). Thus, despite sharing a similar

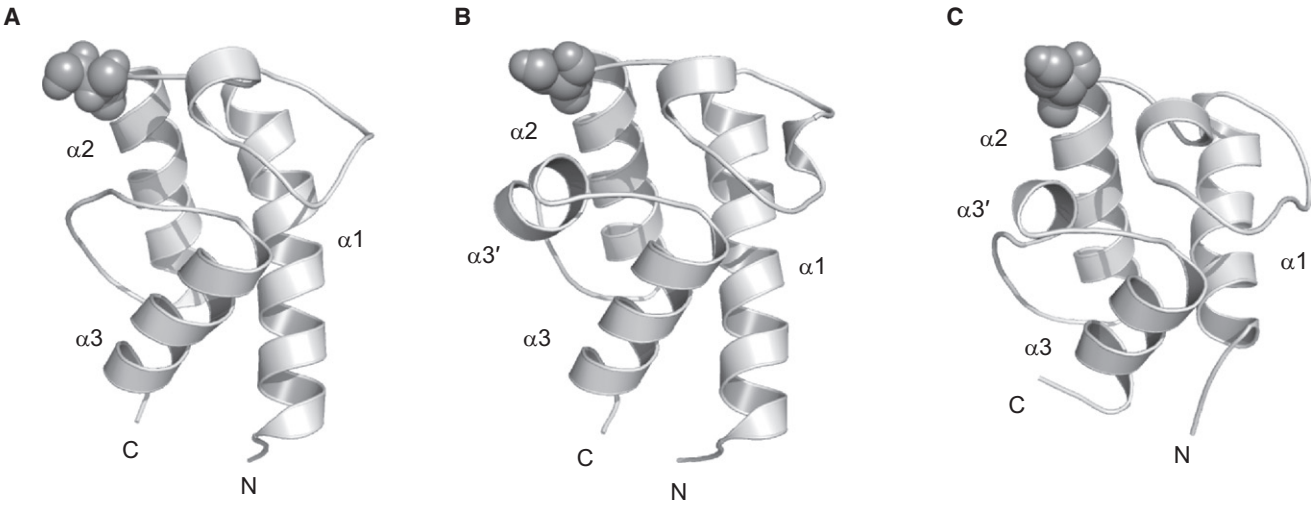

Figure 2. Structure of ACP_6
(A) NOE-based structure of ACP_2 (PDB: 2JU1).
(B) CHESHIRE (chemical shift)-derived structure of ACP_2.
(C) CHESHIRE-derived structure of ACP_6. In each case, the active Ser is displayed in space-filling mode.

biosynthetic logic, there appear to be significant differences in key interdomain interactions within modular PKS and NRPS systems.

RESULTS

Structural Analysis of DEBS *apo* ACP_6

Our initial aim was to collect structural data on ACP_6 in order to characterize any conformational variability induced by interaction with Ppant or attached substrates. For these experiments, discrete ACP_6 was expressed as a C-terminal translational fusion with glutathione-*S*-tranferase (GST), as described previously (Tran et al., 2008), and the GST tag was removed by cleavage with PreScission Protease. In the final protein sample, only the first five residues originate from the expression vector, while residues 6–90 are identical to the DEBS residues 2809–2893 (EryAIII, NCBI reference sequence YP_001102991.1). An analogous construct was used to solve the structure of DEBS ACP_2 (46% sequence identity with ACP_6) (Alekseyev et al., 2007).

The [^{1}H, ^{15}N]-HSQC (heteronuclear single quantum coherence) spectrum of ACP_6 showed 76 of the 83 expected backbone amide signals (see Figure S1A available online). Each residue contributed a single signal to the [^{1}H, ^{15}N]-HSQC spectrum, suggesting that the ACP domain does not adopt multiple conformations in slow exchange on the chemical shift time scale (>0.2 s). Nearly complete backbone assignments for *apo* ACP_6 were obtained from a series of standard triple-resonance NMR experiments. A study of ^{15}N relaxation parameters (Figure S1B–S1D) indicated that the protein backbone was highly structured between residues Met2810 and Gln2886. ^{15}N T_1 and T_2 measurements were used to determine an overall rotational correlation time of 6.0 ± 0.3 ns, consistent with a compact ~80 amino acid domain and confirming that the protein was not prone to self-association (for further details, see the Supplemental Experimental Procedures).

To guide our solution NMR studies, we used the CHESHIRE chemical shift-guided de novo structure prediction protocol (Cavalli et al., 2007) to generate an ensemble of structures for ACP_6. First, we validated this approach by predicting a structure for DEBS ACP_2 from published chemical shifts, which proved highly similar to the NOE-derived structure (2JU1) previously reported (Alekseyev et al., 2007), yielding a root mean square deviation (RMSD) of 1.7 Å between the backbone atom coordinates of residues 19 to 91 (Figures 2A and 2B). Next, we obtained a shift-based structure for ACP_6 (Figure 2C), which over the equivalent residue range (Gln2812 to Gly2884) gave RMSD values of 2.3 Å and 2.4 Å from the CHESHIRE- and NOE-derived structures of ACP_2, respectively. For comparison, a homology model of ACP_6 returned by the I-TASSER server (Zhang, 2009) (Figure S1E) possessed essentially the same fold and showed an RMSD of 2.2 Å from the backbone coordinates of our shift-based structure for ACP_6.

In common with DEBS ACP_2 (Alekseyev et al., 2007) and carrier proteins from other FAS, NRPS, and PKS systems (Kim et al., 2006; Zornetzer et al., 2006; Xu et al., 2001; Roujeinikova et al., 2002; Wong et al., 2002; Li et al., 2003; Findlow et al., 2003; Evans et al., 2008; Frueh et al., 2008), the structure of ACP_6 comprises a right-handed twisted bundle formed by three main α helices (α1, Gln2818–Leu2832; α2, Ser2853–Thr2867; and α3, Val2882–Gly2890), with α1 running antiparallel to α2 and α3. In addition, the linker between α1 and α2 contains a few residues of 3_{10} helix (α2′, Phe2846–Glu2848), while a short α-helix is found between α2 and α3 (α3′, Leu2875–Glu2878). The globular fold of ACP_6 is maintained by interactions between hydrophobic side chains, many of which are conserved in ACP_2 (including Leu2820, Val2840, Leu2849, Ala2856, Leu2859, Leu2863, Thr2867, Leu2871, Leu2875, Leu2885, Ala2886, and Ile2889) (Figure 1B).

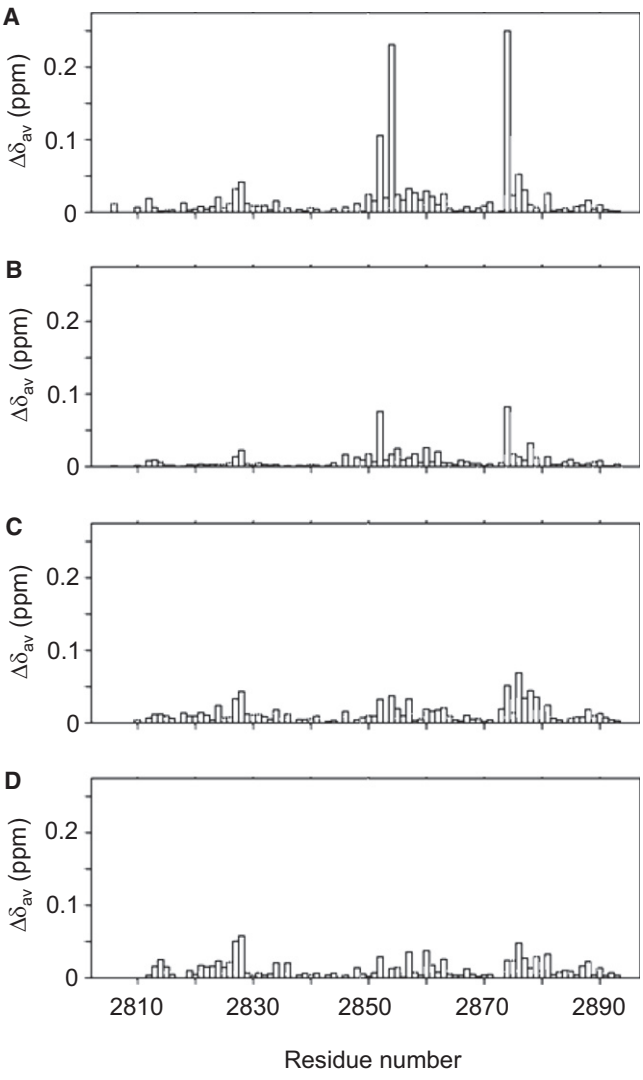

Figure 3. Average $^{1}H/^{15}N$ Chemical Shift Differences Plotted as a Function of Residue Number

(A) *apo* ACP_6 and *holo* ACP_6.
(B) *holo* ACP_6 and butyryl-ACP_6.
(C) *holo* ACP_6 and oxa(dethia) (2*RS*)-methylmalonyl-ACP_6.
(D) *holo* ACP_6 and oxa(dethia) (2*RS*)-2-methyl-3-ketopentanoyl-ACP_6.

Comparative Structural Analysis of *holo* and Acyl-ACP_6

Crump and co-workers recently published the first high-resolution structures of the *apo* and *holo* forms of the same ACP from the type II actinorhodin PKS (act ACP) (Figure 1B) (Evans et al., 2008). Overall, the structures are highly similar: comparison of the [^{1}H,^{15}N]-HSQC spectra of both forms yielded weighted average chemical shift differences ($\Delta\delta_{av}$) of $\leq$0.03 ppm for 90% of the backbone amide resonances. Nonetheless, a detailed analysis revealed that the *holo* protein is subtly contracted relative to the *apo* form, a structural switch induced by interaction between Leu43 on helix α2 (corresponding to ACP_6 Leu2854) and the newly added cofactor. This rearrangement is likely to be responsible for the significant chemical-shift changes observed for nine residues lying along the first half of helix α2, and on helix α3′ (average difference 0.21 ppm, maximum difference 0.5 ppm). On the other hand, chemical shift perturbations to residues Asp41 and Ser42 (corresponding to ACP_6 Asp2852 and Ser2853, respectively) were attributed to the presence of the Ppant tethered to Ser42.

We used this information to interpret the effects of modifying DEBS ACP_6 with Ppant. All residue assignments from the [^{1}H,^{15}N]-HSQC spectrum of *apo* ACP_6 could be transferred to the ACP_6 *holo* protein. Among these, 93% of the chemical shifts matched those in the *apo* domain with weighted average differences of $\leq$0.04 ppm, which we set as the threshold for detecting minor perturbations ($\Delta\delta_{av}$ values are plotted against residue number in Figure 3A and were calculated as in Evans et al., [2008]). These data show that the overall structure of ACP_6 does not change substantially following addition of Ppant. Furthermore, the presence of a single set of ^{1}H-^{15}N correlation peaks in the spectrum of the *holo* protein suggests that, like the *apo* form, it adopts a single conformation (Figure S2A). Of the 11 amino acid residues in ACP_6 that correspond to significantly affected sites in act *holo* ACP, only two show chemical shift changes of comparable magnitude (Asp2852, $\Delta\delta_{av}$ 0.11 ppm; Leu2854, $\Delta\delta_{av}$ 0.23 ppm). By analogy to the act ACP, we attribute the effects at Asp2852 and Leu2854 to covalent attachment of the Ppant arm. The substantial change at Thr2874 (0.25 ppm) and the more minor perturbation to Val2876 (0.05 ppm) are likely to arise from transient interaction with the Ppant group, to which they sit in proximity on the surface of the protein (Figure S2B). Similar prosthetic group dynamics have been reported for type II ACPs (Kim et al., 2006; Li et al., 2003; Wong et al., 2002; Xu et al., 2001; Zornetzer et al., 2006). Taken together, these results suggest that the overall effects of phosphopantetheinylation on the structure are minor.

Next, we evaluated whether ACP_6 might change conformation upon interaction with acyl groups attached to its Ppant arm, as such conformational remodeling has been described for ACPs of both type II PKS (Evans et al., 2009) and FAS (Roujeinikova et al., 2002; Roujeinikova et al., 2007; Wu et al., 2009; Mayo and Prestegard, 1985; Zornetzer et al., 2006). We initially investigated the established substrate mimic butyrate **1** (Tran et al., 2008), an unfunctionalized chain which is bound by both type II PKS (Evans et al., 2009) and FAS (Roujeinikova et al., 2002; Roujeinikova et al., 2007; Wu et al., 2009) ACPs. Butyrate was transferred to the *apo* ACP_6 from its CoA thioester using the broad-specificity phosphopantetheinyl transferase Sfp (Quadri et al., 1998). Detailed comparison of the [^{1}H,^{15}N]-HSQC spectrum of butyryl-ACP_6 with that of the *holo* protein provided no evidence for significant interactions between the domain and the attached substrate (Figure 3B); the majority of $\Delta\delta_{av}$ values were $\leq$0.035 ppm, and only two surface residues in the vicinity of Ser2853 showed larger chemical shift changes (0.076 and 0.082 ppm for Asp2852 and Thr2874, respectively). $\Delta\delta_{av}$ values of this magnitude were observed in a study comparing *holo* and acyl forms of the actinorhodin type II ACP, in which full structure elucidation of the acyl-ACP species confirmed the absence of interaction between the protein and the bound substrates (Evans et al., 2009). To bolster this result, we compared the ^{1}H and ^{13}C NMR spectra of butyryl-pantetheine **2**, $^{13}C_4$-labeled butyryl-CoA **3**, and $^{13}C_4$-butyryl-^{12}C-ACP_6. The $^{13}C_4$-labeled butyryl-CoA **3** was prepared from its pantetheine derivative **4** in a one-pot

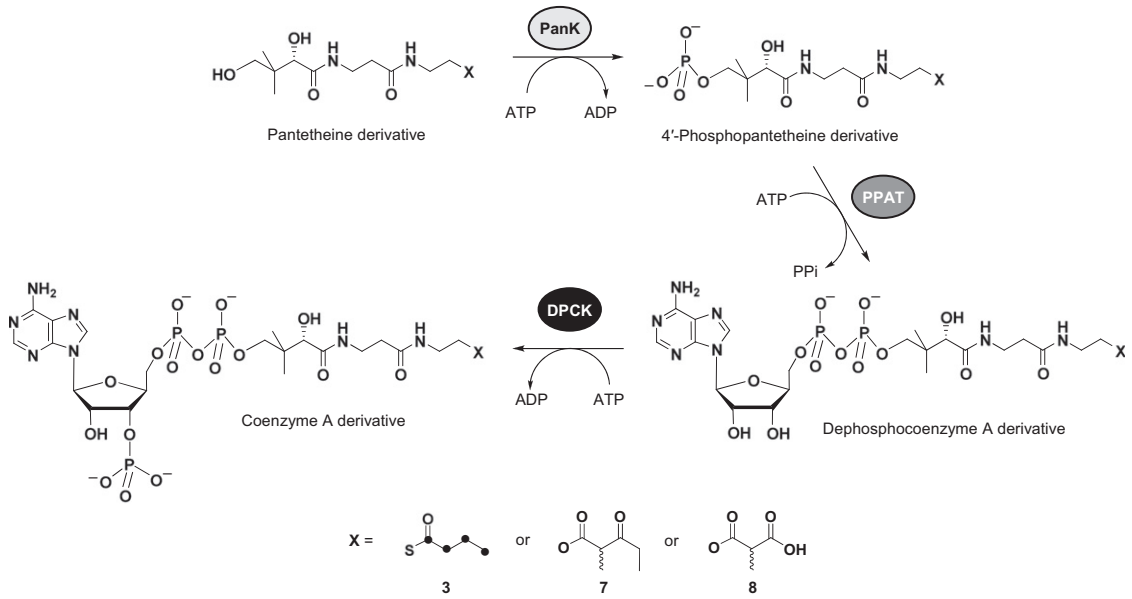

Figure 4. Synthesis of ^{13}C-Butyryl-CoA and Oxa(dethia)-CoA Derivatives in a One-Pot Reaction

The CoA analogs are generated from the corresponding pantetheine derivatives using pantothenate kinase (PanK), phosphopantetheine adenyltransferase (PPAT), and dephosphocoenzyme A kinase (DPCK). **X** corresponds to ^{13}C-labeled butyrate, oxa(dethia)-(2*RS*)-methylmalonate, and oxa(dethia)-(2*RS*)-2-methyl-3-ketopentanoate.

reaction using recombinant pantothenate kinase (PanK), phosphopantetheine adenyltransferase (PPAT) and dephosphocoenzyme A kinase (DPCK) (Nazi et al., 2004) (Figure 4). (This synthesis and that of ^{12}C- (**2**) and $^{13}C_4$-butyryl-pantetheine **4** are described in the Supplemental Experimental Procedures.) Although minor chemical shift changes were observed between the three butyrate species (Table 1), these minimal perturbations confirm the absence of significant, persistent interactions between the acyl chain and the ACP domain. These results strengthen the view that unlike type II FAS and PKS ACP domains, type I ACPs show no significant affinity for hydrophobic chain assembly intermediates (Wattana-Amorn et al., 2010; Ploskon et al., 2008).

As butyrate lacks the complex functionality of the natural heptaketide intermediate attached to ACP_6, we also investigated chemical shift effects caused by two more native substrate analogs. For this we chose a diketide mimic ([2*RS*]-2-methyl-3-ketopentanoate), as well as a racemic analog of the natural chain extension unit (2*S*)-methylmalonate (Marsden et al., 1994) (Figure 4). Both compounds were synthesized in hydrolytically stable form, taking advantage of recently developed methodology for the preparation of oxa(dethia)pantetheine (Tosin et al., 2010) and coenzyme A analogs (Tosin et al., 2009). In brief, (2*RS*)-2-methyl-3-ketopentanoate and (2*RS*)-methylmalonate were synthesized as their oxa(dethia) pantetheine esters (**5** and **6**, respectively) (Supplemental Experimental Procedures) and then converted to the corresponding CoA compounds (**7** and **8**) using PanK, PPAT, and DPCK (Nazi et al., 2004). Transfer of these acyl-phosphopantetheines to ACP_6 was achieved using Sfp. Again, [^{1}H,^{15}N]-HSQC experiments revealed no significant interactions between the acyl groups and the protein (Figures 3C and 3D). It has been recently reported that ACP_6 can collaborate in vitro with a didomain consisting of a ketosynthase (KS) and an acyltransferase (AT) to synthesize 2-methyl-3-ketodiketide-ACP_6 (Valenzano et al., 2009). By reductive trapping with $NaBH_4$, the methyl group was found to be configurationally

Table 1. Chemical Shift Changes Observed in the Series Butyryl-pantetheine, $^{13}C_4$-Labeled Butyryl-CoA, $^{13}C_4$-Butyryl-^{12}C-ACP_6, $^{13}C_4$-Butyryl-^{12}C-ACP_6 + TE (titration), and $^{13}C_4$-Butyryl-^{12}C-ACP_6-TE (Relative to Butyryl-CoA)

C4 (CH_3 site)	δ(H)/ppm	δ(C)/ppm	Δδ(H)/ppm	Δδ(C)/ppm
Butyryl-pantetheine	0.927	15.43	0.043	−0.06
Butyryl-CoA	0.884	15.49	0	0
Butyryl-ACP_6	0.849	15.66	−0.035	0.17
Butyryl-ACP_6/TE (titration)	0.854	15.66	−0.03	0.17
Butyryl-ACP_6-TE	0.849	15.66	−0.035	0.17
C3 (CH_2 site)				
Butyryl-pantetheine	1.663	21.82	0.055	0.13
Butyryl-CoA	1.608	21.69	0	0
Butyryl-ACP_6	1.58	21.73	−0.028	0.04
Butyryl-ACP_6/TE (titration)	1.58	21.73	−0.028	0.04
Butyryl-ACP_6-TE	1.58	21.82	−0.028	0.13
C2 (CH_2 site)				
Butyryl-pantetheine	2.635	48.22	0.067	0.09
Butyryl-CoA	2.568	48.13	0	0
Butyryl-ACP_6	2.528	48.22	−0.04	0.09
Butyryl-ACP_6/TE (titration)	2.528	48.22	−0.04	0.09
Butyryl-ACP_6-TE	2.528	48.22	−0.04	0.09

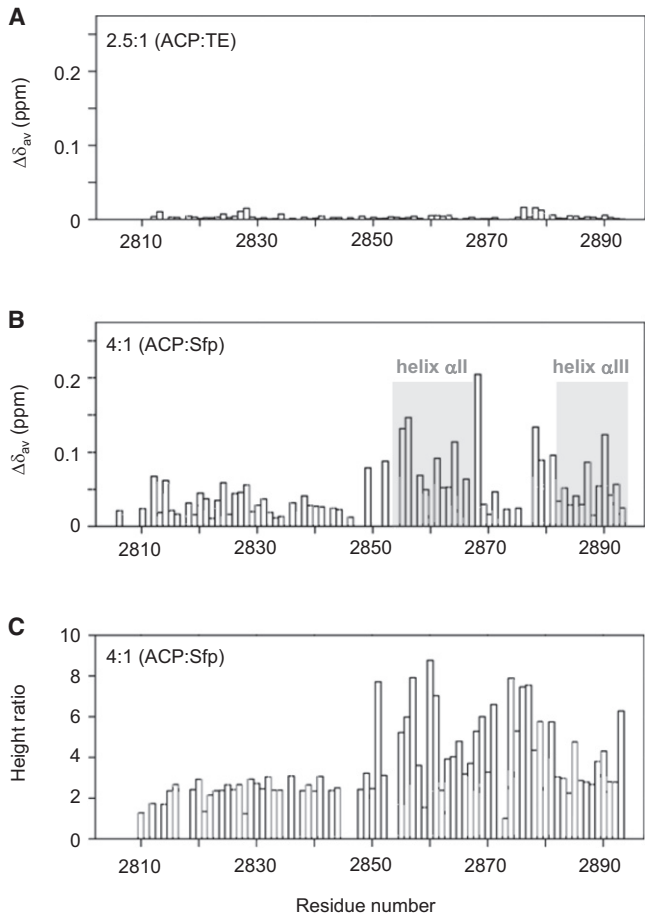

Figure 5. Analysis for Binding between Butyryl-ACP$_6$ and TE in *trans*

(A) Average $^1H/^{15}N$ chemical shift differences for butyryl-ACP$_6$ in the presence and absence of TE (S3030A).

(B) Average $^1H/^{15}N$ chemical shift differences for ACP$_6$ (S2853A) in the presence and absence of Sfp.

(C) [^1H, ^{15}N]-HSQC resonance height ratios for ACP$_6$ (S2853A) in the presence and absence of Sfp.

stable, a feature which was attributed to interaction of the chain with ACP$_6$. However, this hypothesis is inconsistent with the lack of such contacts in our experiments. We suggest instead that stabilization may arise through an interface with the KS-AT didomain, but, nevertheless, the exact basis for this discrepancy remains to be determined.

Interaction between DEBS Acyl-ACP$_6$ and TE in *trans*

We previously used in vitro enzymatic assays to show that a discrete TE can catalyze release of butyrate **1** from isolated ACP$_6$, albeit inefficiently (pseudo first order rate constant k = 0.00101 ± 0.00002 s^{-1}) (see Supplemental Experimental Procedures). Furthermore, comparative analysis of the interaction between the TE and various forms of ACP$_6$ (*apo*, *holo*, and butyryl) by isothermal titration calorimetry (ITC) and surface plasmon resonance (SPR) suggested that the binding by the TE was limited to the Ppant arm and/or the acyl chain. We aimed to confirm these results using NMR, monitoring butyryl-^{15}N-ACP$_6$ (500 μM) in the presence of the TE (200 μM), suppressing catalytic turnover by employing an active site mutant of the TE (Ser3030Ala). This experiment was carried out under conditions identical to the previous enzymatic assays (Tran et al., 2008), with the exception that the spectra were acquired at 25°C instead of 37°C; crucially, we confirmed that the wild-type TE still catalyzed turnover of butyryl-ACP$_6$ at this lower temperature (k = 0.00076 ± 0.00003 s^{-1}).

We looked for evidence of binding to TE (S3030A) in the [^1H,^{15}N]-HSQC spectrum of the ACP$_6$ domain, including significant changes from the chemical shifts of butyryl-ACP$_6$ alone which would identify interface residues, and line broadening effects that might indicate formation of an ACP/TE protein-protein complex. We observed neither (Figure 5A), even though the final concentrations of both domains were far in excess of the K_D for binding measured by ITC (18 ± 1 μM) (Tran et al., 2008). These negative results support the idea that the TE can interact with ACP-tethered substrates in the absence of contact with the ACP domain itself. We also carried out analogous titrations with nonhydrolyzable (*2RS*)-2-methyl-3-ketopentanoate (derived from **7**, Figure 4) bound to ACP$_6$ (molar ratios ACP$_6$:TE 4:1, 2:1 and 1:1). Again, we found no evidence for persistent interactions between the TE and the ACP$_6$ domain (Figure S3A).

To demonstrate that we could detect formation of a protein-protein complex using our NMR methodology, we analyzed the interaction between *apo* ACP$_6$ and the PPTase Sfp. We had shown previously by site-directed mutagenesis of ACP$_6$ coupled with assays in vitro, that Sfp interacts directly with ACP$_6$, contacting several residues along the length of helix α2 (Weissman et al., 2006). However, we were unable to analyze the interaction with wild-type *apo* ACP even in the absence of added Mg^{2+} and CoA cofactors, as conversion to the *holo* form in the presence of Sfp was rapid. To prevent this reaction, we replaced the active site Ser2853 of ACP$_6$ with Ala (Koglin et al., 2006); [^1H,^{15}N]-HSQC experiments showed that the mutation is isomorphous, leaving the domain essentially unchanged except in the immediate vicinity of residue 2853 (Figure S3B). From preliminary experiments, we determined that it was necessary to premix Sfp with equimolar quantities of CoA and Mg^{2+}; addition of Sfp in the absence of either CoA or Mg^{2+} resulted in poor stability of the PPTase, as well as nonspecific binding to ACP$_6$ (S2853A). We then acquired [^1H,^{15}N]-HSQC spectra of ACP$_6$ (S2853A) as Sfp was titrated into the solution (ACP$_6$ [S2853A]:Sfp molar ratios of 1:0, 4:1, 2:1, and 1:1). For technical reasons we assigned only 87% of the expected signals for ACP$_6$ (S2853A), but a comparison of spectra acquired in the absence and presence of Sfp allowed us to identify a set of amino acids at the intermolecular interface ($\Delta\delta_{av}$ [ppm] values are plotted against residue number in Figure 5B). Consistent with our mutagenesis results (Weissman et al., 2006), interface residues were identified on helix α2, but additionally on helix α3′, α3, and the intervening loops; little interaction was observed with the N-terminal half of the protein. In addition, analysis of peak intensities showed that all ACP$_6$ (S2853A) resonances were broadened in the presence of Sfp, as expected when a small protein participates in a complex (MW Sfp = 22 kDa) (Figure 5C). This analysis acts as a positive control for our TE binding experiments, demonstrating that our data accurately reflect the absence of direct contact between the TE and ACP$_6$ domains.

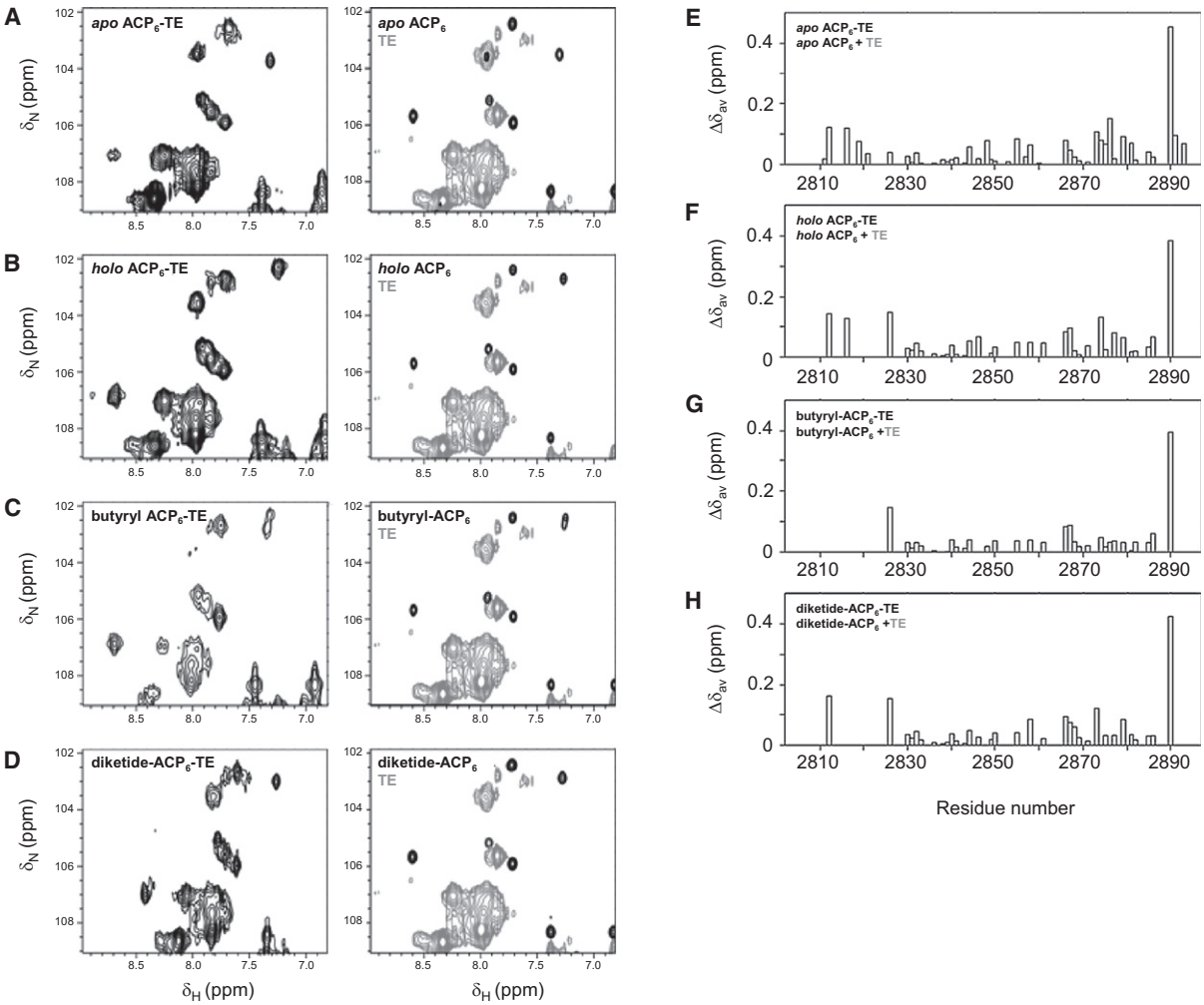

Figure 6. Interactions of DEBS Acyl-ACP$_6$ and TE in *cis*

Expanded view of the [^{1}H, ^{15}N]-HSQC spectra of (A) *apo* ACP$_6$-TE and *apo* ACP$_6$ + TE, (B) *holo* ACP$_6$-TE and *holo* ACP$_6$ + TE, (C) butyryl-ACP$_6$-TE and butyryl-ACP$_6$ + TE, and (D) oxa(dethia)-(2*RS*)-2-methyl-3-ketopentanoyl-ACP$_6$-TE (diketide-ACP$_6$-TE) and diketide-ACP$_6$ + TE. Average ^{1}H/^{15}N chemical shift differences plotted as a function of residue number for (E) *apo* ACP$_6$-TE and *apo* ACP$_6$ + TE, (F) *holo* ACP$_6$-TE and *holo* ACP$_6$ + TE, (G) butyryl-ACP$_6$-TE and butyryl-ACP$_6$ + TE, (H) diketide-ACP$_6$-TE and diketide-ACP$_6$ + TE.

Interaction between DEBS Acyl-ACP$_6$ and TE in *cis*

Transfer of butyrate **1** between ACP$_6$ and TE is extremely rapid when the domains are covalently linked (Tran et al., 2008). Thus, it remained a formal possibility that the domains assemble into a complex at the high effective concentrations produced by direct tethering within the DEBS multienzyme by a short (11 residue) linker. To evaluate this question directly, we compared the [^{1}H,^{15}N]-HSQC spectra of *apo* ^{15}N-ACP$_6$, His$_6$-tagged *apo* ^{15}N-ACP$_6$-TE and His$_6$-tagged ^{15}N-TE. Due to overlap with the TE signals, we were only able to reassign 42 of 76 ACP resonances in the spectrum of the ACP$_6$-TE didomain, but their frequencies were essentially unchanged relative to the discrete protein (Figures 6A and 6E). The major exceptions were for residues at or near the direct covalent linkage between the two domains. We also observed a small extent of line broadening for the ACP signals. The magnitude of this change is not consistent with formation of a tight complex between the proteins but instead indicates that tethering to another domain moderately restricts the mobility of the ACP. Similarly, ACP residues in the *holo* ACP$_6$-TE (34 signals) overlaid well with those from the discrete *holo* ACP$_6$ (Figures 6B and 6F), in that both were shifted to the same minor extent from their *apo* forms.

We next extended this analysis to two acyl-ACP$_6$ species, butyryl-ACP$_6$-TE (S3030A) and oxa(dethia)-(2*RS*)-2-methyl-3-ketopentanoyl-ACP$_6$-TE (S3030A). In both cases, the detectable signals from the ACP domain (31 and 33, respectively) overlaid well with those of equivalently modified discrete ACP domains (Figures 6C, 6D, 6G, and 6H; Figure S4). We had anticipated that the ACP domain might experience additional motional restraints when the attached substrate bound into the TE active site, leading to a broadening of resonances relative to those in spectra of the tethered *holo* domain. Intriguingly, however, the signals from both acyl-ACP-TE species had similar linewidths to those from the *apo* and *holo* ACP-TE constructs. This observation suggested that only the extreme Ppant-attached end of the substrate becomes restricted on

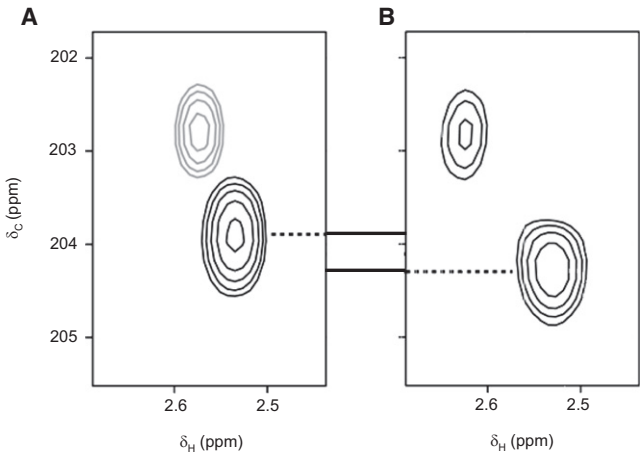

Figure 7. Binding of TE (S3030A) to the C1 Carbonyl of Butyryl-ACP$_6$
(A) H(C)CO spectrum of $^{13}C_4$-butyryl-CoA (gray) and $^{13}C_4$-butyryl-^{12}C-ACP$_6$ (black).
(B) H(C)CO spectrum of $^{13}C_4$-butyryl-^{12}C-ACP$_6$-TE (S3030A).

binding to the TE, and consequently that the ACP itself remains relatively mobile.

To obtain direct evidence for this mode of binding, we generated uniformly labeled $^{13}C_4$-butyryl-^{12}C-ACP$_6$-TE (S3030A) and compared its behavior to $^{13}C_4$-butyryl-^{12}C-ACP$_6$ using a [^{1}H, ^{13}C]-HSQC experiment, which detects carbon nuclei which are directly attached to hydrogen atoms. The chemical shifts for C2, C3, and C4 of butyrate matched closely in both samples, indicating the absence of an interaction with the TE in the didomain (Table 1; Figure S5). To directly interrogate the remaining carbonyl carbon (C1), we carried out a modified H(CA)CO experiment (Supplemental Experimental Procedures), which revealed a ^{13}C chemical shift change of 0.33 ppm, consistent with binding to the TE (compare Figures 7A and 7B). To further confirm this result, we analyzed $^{13}C_4$-butyryl-^{12}C-ACP$_6$ (initial concentration of 1.25 mM in the presence of increasing concentrations of TE$_{S3030A}$ (final ACP$_6$:TE molar ratios of 1:0, 1:0.25, 1:0.5, and 1:1). In agreement with the result for the didomain, there were no significant chemical shift changes for aliphatic sites at any TE concentration (Table 1). Unexpectedly, we also failed to detect a change in shift for the carbonyl ^{13}C resonance, even at 1:1 ACP$_6$:TE (final concentration of both species 0.5 mM). However, upon increasing the concentration of the 1:1 mixture to 3.1 mM in each species, we detected a carbonyl ^{13}C shift of 0.18 ppm in the same direction as that found for the acyl-didomain (Figure S5). Crucially, the magnitude of the shift changes in both the didomain and titration experiments substantially exceeded the sample-to-sample variation observed in spectra of discrete $^{13}C_4$-butyryl-ACP$_6$ preparations. (For additional discussion of this experiment and its interpretation, see the Supplemental Experimental Procedures.) Taken together, these data show that within the context of the multienzyme the interaction between butyryl-ACP$_6$ and the TE complex is minimal and is likely to be limited to the C1 carbonyl group of the acyl chain (although interactions with the Ppant arm cannot at present be ruled out). This finding implies that the TE domain should exhibit broad substrate tolerance in the acylation reaction, an expectation confirmed by analysis in vitro of ACP$_6$-TE with a range of substrate analogs varying in both chain length and functionality (Aggarwal et al., 1995).

Although somewhat unexpected, these results are also entirely consistent with two recent studies on substrate binding by isolated DEBS TE (Wang and Boddy, 2008) and the homologous TE from the pikromycin (Pik) PKS (Akey et al., 2006; Giraldes et al., 2006). The data obtained respectively from site-directed mutagenesis and polyketide-based affinity labeling show a lack of direct, specific contact between the TE domains and the acyl chains, both in the substrate loading step (as shown for DEBS TE), and prior to the cyclization reaction (Pik TE). No evidence has been adduced for substrate recognition via specific hydrogen bonds or by a protein surface of complementary shape, using a range of substrate analogs including a near-native pentaketide mimic of pikromycin (Akey et al., 2006; Giraldes et al., 2006). These findings are highly relevant to the data reported here, as it could have been argued that extensive interaction between the TE and the incoming substrate might provoke a conformational change in the TE domain, exposing a new interface to the upstream ACP. On the contrary, the structures of unbound and substrate-modified Pik TE were found to be identical (Giraldes et al., 2006). To explain the ability of the TEs to catalyze macrolactonization using both ends of the substrate, Akey and co-workers identified a ''hydrophilic barrier'' at the exit site of the Pik TE substrate channel (Akey et al., 2006). This region forces the substrate to curl back upon itself, causing its distal end to approach the active site Ser. Chain release via a classical tetrahedral intermediate is then facilitated by an oxyanion hole, provided in the case of the PikTE by the NH group of Gly149. We note that this interaction with the C1 carbonyl group, one of only two direct contacts demonstrated to date between the PikTE and a substrate mimic, is precisely that observed between DEBS TE and butyrate.

DISCUSSION

Biosynthesis of polyketide and nonribosomal peptides requires the coordinated action of minimally tens of individual catalytic domains, housed within large multienzyme subunits. The reactions occur on substrates attached in thioester linkage to the Ppant prosthetic group of integral carrier proteins. Consequently, these small, noncatalytic domains have taken center stage in efforts to elucidate assembly-line production of natural products (Lai et al., 2006; Weissman and Müller, 2008). X-ray crystallographic studies of both PKS (Tang et al., 2006) and NRPS (Samel et al., 2007; Tanovic et al., 2008) have shown that the distance between successive catalytic domains exceeds the reach of a static Ppant arm, implying that the entire carrier proteins must relocate within the complexes to deliver their cargo. NMR has been arguably even more informative, revealing that in the case of the tyrocidine NRPS, this dynamic theme extends to the structure of the PCP domain itself (Koglin et al., 2006). Conformational rearrangements through interaction with Ppant and by extension with substrate appear to optimize PCPs for complex formation with specific partners, in principle dictating the sequence of interactions during each chain extension cycle. The catalytic domains may contribute an additional layer of regulation, as an NRPS TE has been shown to flip

between open and closed conformations, alternately exposing and concealing its Ppant binding site (Frueh et al., 2008).

Similar control features have also been proposed to operate in PKS systems (Frueh et al., 2008; Weissman and Müller, 2008; Kapur and Khosla, 2008; Lai et al., 2006), and this remains an appealing mechanism. However, the data reported here strongly support the idea (Tran et al., 2008) that at least some ACP-based communication is facilitated solely by the proximity of the ACP and its partner domains within the multienzyme complex. In the case of the interaction between acyl-ACP and the TE domain, chain transfer can occur efficiently in the absence of a protein-protein interface, with contact limited to the substrate. These results are entirely consistent with the finding that the DEBS TE can partner effectively with multiple, noncognate ACP domains in engineered PKS systems in vivo (Cortés et al., 1995; Martin et al., 2003). In addition, our data provide no evidence for conformational heterogeneity within a typical ACP domain, whether induced through contacts with Ppant or acyl substrates. However, as our studies were carried out with the chain extension unit methylmalonate and short chain polyketide mimics, we cannot yet rule out that PKS ACPs interact with longer, more highly functionalized intermediates. Nonetheless, our results clearly demonstrate that conformational switching is not absolutely required for effective communication with the TE domain.

This means of cooperation may also apply to ketoreductase domains, which exhibit a relaxed specificity toward their ACP partners (Chen et al., 2007). In contrast, both KS and AT domains show a preference for particular ACPs (Wong et al., 2010; Kim et al., 2004; Chen et al., 2006), a specificity that in the case of the KSs can be influenced by site-directed mutagenesis at ACP surface residues (Alekseyev et al., 2007). These results are consistent with formation of a specific protein-protein interface between the ACP domain and the KS and AT enzymes, which together constitute the core of a functional PKS module. Thus, several modes of ACP-centered communication appear to operate simultaneously in type I PKS systems. This finding accords with a proposed mechanism for the evolution of modular PKSs (Jenke-Kodama et al., 2006), in which catalytic domains, with the exception of KSs, are added, deleted, or exchanged into a given module by homologous recombination within the interdomain linker regions. From this perspective, a model in which at least some of the resulting ACP partnerships are facilitated by proximity instead of optimized protein-protein interfaces is attractive.

As the interaction between the ACP and TE domains is proximity driven, how then is chain transfer controlled so that the appropriate level of processing is achieved within the chain extension module before the substrate is handed on to the TE domain? Several possible mechanisms can be envisaged. For example, the TE may regulate access to its active site via a mobile flap, as demonstrated for TEs from the enterobactin (Frueh et al., 2008) and surfactin (Bruner et al., 2002) NRPSs. However, the X-ray structures of the TEs from the DEBS (Tsai et al., 2001) and Pik (Tsai et al., 2002) PKSs provide no direct evidence that these domains can adopt the requisite open and closed conformations, although studies of dynamics in solution may yet reveal greater conformational flexibility. Alternatively, chain transfer to the TE may not be tightly regulated, but off-loading may occur relatively slowly. According to this "retardation control" mechanism, the subsequent chain extension intermediate would stall within the upstream module, providing adequate time for all reductive reactions to occur (Hong et al., 2009). A final possibility is suggested by a recent electron microscopy study of type I animal FAS, a multienzyme which is likely to share architectural features with modular PKS (Smith and Tsai, 2007; Weissman, 2008). FAS carries out an analogous set of reactions to a fully reducing PKS module, using sets of domains organized into two independent reaction chambers. The domains are deployed iteratively until the appropriate chain length is reached, and then the mature fatty acid is liberated by the terminal TE domain. Catalysis of substrate loading and chain extension require asynchronous closing of the two reaction chambers, a global conformational rearrangement which simultaneously appears to block access of the TE to the ACP (Brignole et al., 2009). Whether this exclusion mechanism also operates in modular PKS to control the timing of chain release will only be revealed by high-resolution data on an intact module, combined with dynamical information.

An important motivation for studying PKS systems is to improve our ability to genetically manipulate these multienzymes toward the production of novel metabolites, an approach referred to as combinatorial biosynthesis (Weissman and Leadlay, 2005). One of the most successful strategies has been to exchange specific catalytic domains within and between different synthases. While several hundred new compounds have been generated to date by this method, hybrid assembly lines are often kinetically compromised relative to their parents, produce undesirable mixtures of products because specific domains fail to act, or are simply nonfunctional. Although there are likely to be several explanations for these results, our data support the idea that the failure to maintain proper spatial relationships between the ACP and its partners may alone account for a number of these findings (Hans et al., 2003). This is encouraging, because it implies that structural data on representative modules which reveal the relative dispositions of the ACP and catalytic domains will substantially advance efforts to make such engineering routine.

SIGNIFICANCE

Biosynthesis of complex polyketide metabolites requires the coordinated action of minimally tens of individual protein domains housed within gigantic multienzyme assembly lines (modular polyketide synthases [PKSs]). The central players in the pathways are small, noncatalytic acyl carrier protein (ACP) domains, to which the growing polyketide chains are tethered in covalent linkage. Little is known about how the catalytic domains communicate with acyl-ACPs or how these interactions are controlled, which are features that must be preserved if efforts to generate novel polyketide analogs by genetic engineering (so-called "combinatorial biosynthesis") are to be successful. Based on similarities in biosynthetic logic between PKSs and the nonribosomal peptide synthetases (NPRSs), it has been suggested that the choice of catalytic partner in modular PKS is guided by substrate-induced conformational switching in the ACP domain. That is, contacts with the substrate modulate the

structure of the ACP so that it is primed to form a complex with a specific partner. We have addressed this hypothesis directly by using a model system comprising an ACP domain and its adjacent thioesterase (TE), from the PKS responsible for erythromycin biosynthesis. Using a combination of NMR, site-directed mutagenesis, chemical synthesis, and site-specific protein labeling, we demonstrate that the ACP adopts a single conformation in solution and does not interact substantially with either attached phosphopantetheine cofactor or substrate. In addition, effective chain transfer between the ACP and the TE occurs in the absence of a defined protein-protein complex, and instead recognition focuses on the carbonyl group of the acyl chain. Taken together, these findings argue against the proposed programming model, revealing a fundamental mechanistic difference between modular PKS and NRPS systems.

EXPERIMENTAL PROCEDURES

Biological Materials and General Methods

All chemicals were reagent grade. Ampicillin, kanamycin, chloramphenicol, Bradford reagent, glutathione, Tris (tris hydroxymethylaminomethane), and EDTA (ethylenediamine tetraacetic acid) were purchased from Sigma. IPTG (isopropyl-β-D-thiogalactopyranoside) and dithiothreitol (DTT) were obtained from Melford Laboratories, Ltd. NaH_2PO_4 and NaCl were purchased from Fischer Chemicals. Complete protease inhibitor cocktail tablets were obtained from Roche Molecular Biochemicals. ^{15}N-labeled Celtone, ^{13}C-labeled glucose, and ^{15}N-labeled ammonium chloride were obtained from Spectra Stable Isotopes. Strain *Escherichia coli* BL21-CodonPlus-RP was obtained from Stratagene. Standard procedures for DNA isolation and manipulation were performed as described previously (Sambrook and Russell, 2001). Restriction endonucleases and T4 DNA ligase were obtained from New England Biolabs. Mutagenic PCR was carried out using the QuickChange Site-Directed Mutagenesis Kit (Stratagene), while standard PCR reactions were performed with Pfu polymerase (Stratagene). Synthetic oligonucleotides were purchased from Invitrogen, and automated DNA sequencing was carried out on double-stranded DNA templates using an automated ABI Prism 3700 DNA Analyzer (Applied Biosystems).

Chemical Materials and General Methods

NMR spectra were recorded at 300 K using Bruker DPX-400, Avance 400 QNP and Avance 500 spectrometers. For ^{1}H- and ^{13}C-NMR the chemical shifts are reported relative to the solvent signal ($CDCl_3$ δ_H 7.26, D_2O δ_H 4.80, CD_3OD δ_H 3.31, $CDCl_3$ δ_C 77.0, and CD_3OD δ_C 49.0). The ^{1}H- and ^{13}C-NMR signals were unequivocally assigned with the aid of g-COSY, DEPT and HMQC. All chemicals were purchased from Sigma-Aldrich (unless otherwise stated). The reaction solvents were dried and distilled according to the methods of Burfield and Smithers (1983). HPLC purification was carried out on a semi-preparative Phenomenex Synergi polar RP column (250 × 10.0 mm, 4 μm) using an Agilent HP 1100 HPLC; mixtures of water and acetonitrile (with addition of FA when stated) were used with a flow rate of 2.5 ml min^{-1} with an elution gradient starting from 100% water and linearly increasing to 100% acetonitrile over 30 min (unless otherwise stated), with UV detection set at 254, 280, and 210 nm. LR- and HR-ESI-MS spectra of synthetic intermediates were obtained from an Agilent HP1100 HPLC coupled to a Finnigan MAT LCQ mass spectrometer (fitted with an ESI source) and a Waters LCT Premier mass spectrometer respectively. HR-ESI-MS analysis of final purified products was performed on a Thermo Electron LTQ-Orbitrap (run in positive ionization mode, scanning from m/z 100 to 1800, with the FTMS analyzer resolution set at 60K).

Design of Expression Constucts

DEBS ACP_6 was amplified as a BamHI-EcoRI fragment from plasmid pKJW191R (Weissman et al., 2004) using primers ACP6NBam and ACP6CEco (all primer sequences are provided in the Supplemental Experimental Procedures). DEBS TE was amplified as a BamHI-EcoRI fragment from plasmid pKJW191R using primers TENBam and TECEco. The PCR products were digested with BamHI and EcoRI and ligated into pGEX-6P-1, yielding plasmids pGEX-ACP_6 and pGEX-TE, repsectively. The construction of plasmids pKJW63 (C-terminally His_6-tagged TE), pACP-TEHis, and pSfp was described previously (Tran et al., 2008). Single serine to alanine active site mutations were introduced into ACP_6 by Quickchange site-directed mutagenesis (Stratagene), using the primers ACPsS2853A and ACPaS2853A to generate pGEX-AC-P_6(S2853A), and into the TE and the ACP_6-TE didomain using primers TEsS3030A and TEaS3030A, yielding pGEX-TE(S3030A) and pACP_6-TE (S3030A). The fidelity of all PCR and mutagenesis reactions was confirmed by sequencing. The sequences of proteins created in this study are provided in the Supplemental Experimental Procedures. Cloning of PanK, PPAT, and DPCK (Nazi et al., 2004) is described in detail in Tosin et al., (2009).

Expression of Labeled and Unlabeled Protein Samples for NMR analysis

GST-tagged TE (S3030A) and N-terminally His_6-tagged Sfp were expressed in *Escherichia coli* BL21 (DE3) CodonPlusRP (Stratagene) for 5 hr in LB medium supplemented with 50 mg ml^{-1} chloramphenicol and 100 mg ml^{-1} carbenicillin (TE [S3030A]) or 50 mg ml^{-1} kanamycin (His_6-tagged Sfp) at 30°C, after induction with 0.2 mM IPTG. TE (S3030A) was subsequently released from GST by limited proteolysis with PreScission Protease as described in the Supplemental Experimental Procedures. To obtain uniformly labeled ^{15}N-labeled ACP_6, ACP_6 (S2853A), ACP_6-TE_{His} (S3030A), and TE_{His}, cells were grown for 16 hr at 22°C in M9 minimal medium containing ^{15}N-labeled ammonium chloride (Spectra Stable Isotopes) (and 1% ^{15}N-labeled Celtone for ACP_6 [S2853A]), in the presence of the appropriate antibiotics, after induction with 0.2 mM IPTG. ^{13}C,^{15}N-labeled ACP_6 was obtained using the same medium, but supplemented additionally with ^{13}C-labeled glucose. All constructs were purified as described in the Supplemental Experimental Procedures, and the protein identities confirmed by HPLC-MS (Figures S6A, S6F, and S6H).

Enzymatic Synthesis of CoA Analogues

Nonhydrolyzable diketide pantetheine, nonhydrolyzable methylmalonyl pantetheine, and ^{13}C-butyryl-pantetheine were synthesized as described in the Supplemental Experimental Procedures. Five millimolar pantetheine derivative was dissolved in reaction buffer (20 mM KCl, 10 mM $MgCl_2$, 20 mM ATP, and 50 mM Tris.Cl [pH 7.5]), and the reaction was initiated by addition of 5 mg PanK, 5 mg PPAT, and 5 mg DPCK (Nazi et al., 2004; Tosin et al., 2009). Reaction mixtures were incubated at 22°C for 3 hr, and the reactions were monitored for completion by HPLC-MS analysis (Figures S6M, S6N, and S6O) using a Polar RP 80 Å column (250 × 2.00 mm) with a linear gradient (25%–95% acetonitrile/water containing 0.1% trifluoroacetic acid), over 20 min at a flow rate of 0.3 ml min^{-1}. Further information on analysis by HPLC-MS is provided in the Supplemental Experimental Procedures.

Phosphopantetheinylation and Acylation of ACP_6 and ACP_6-TE_{S3030A}

One millimolar ACP_6 or ACP_6-TE_{His} (S3030A) was incubated with 31 nM Sfp, in buffer (50 mM NaPi [pH 7.0], 10 mM $MgCl_2$, 5 mM DTT, and 2 mM CoASH [or acyl-CoASH]) in a 2 ml reaction volume. Reactions were allowed to proceed at 22°C for 2 hr, before purification by gel filtration using a Superdex 75 size exclusion column (Amersham) in PBS (50 mM sodium phosphate buffer [pH 8.0], 150 mM NaCl). To confirm quantitative modification (Figures S6B–E, S6G, and S6I– S6L), samples were subsequently analyzed by HPLC-MS using a reverse phase column (Vydac, Protein C4, 5 μm, 250 × 2.0 mm, 300 Å) with a linear gradient (25%–95% acetonitrile/water containing 0.1% trifluoroacetic acid), over 20 min at a flow rate of 0.3 ml min^{-1}.

Protein NMR Spectroscopy

Typical samples were prepared containing 1 mM of ^{15}N or ^{15}N/^{13}C-labeled protein in a solution of 50 mM sodium phosphate and 150 mM sodium chloride (pH 8.0), with 20 μM 3,3,3-trimethylsilylpropionate (TSP), protease inhibitor cocktail (Roche), and 10% D_2O, to a final volume of 500 μl in 5 mm Ultra-Imperial grade NMR tubes (Wilmad). [^{1}H, ^{15}N]-HSQC, HNCA, HN(CO)CA, HNCO, HNCACB, CBCA(CO)NH, ^{15}N-NOESY-HSQC, ^{15}N-HSQC-NOESY-HSQC, and ^{15}N-relaxation and modified H(CA)CO spectra were recorded using standard procedures (Palmer et al., 2006) at 20°C (titration experiments), 25°C (^{15}N relaxation experiments), or 35°C on Bruker DRX500, DRX600, and

DRX800 spectrometers. For further details of acquisition, processing, and analysis, see the Supplemental Experimental Procedures.

Modeling of the ACP_6 Structure

The CHESHIRE (Cavalli et al., 2007) de novo structure determinations for ACP_2 and ACP_6 were performed by generating 40,000 low-resolution structures using a fragment replacement procedure, followed by energy minimization and chemical shift guided selection of the 250 best matches for further refinement. Six thousand five hundred structures were generated in the refinement stage, entailing repeated rounds of random selection of structures for simulated annealing and subsequent updating of the list of high-scoring structures. The 10 best scoring structures were selected as the final ensemble. Over residues 19–91, the backbone RMSD for the ACP_2 ensemble was 0.4 Å. Over residues 2812–2884, the RMSD for the ACP_6 ensemble was 1.4 Å; this comprised a low energy family of seven structures (RMSD 0.5 Å) and a higher energy group of three structures (RMSD 0.4 Å). In each case, the lowest energy conformation was taken to be representative. A sequence-based homology model of ACP_6 was obtained from the I-TASSER server (Zhang, 2009) (http://zhang.bioinformatics.ku.edu/I-TASSER/) using the default settings.

Interaction of DEBS acyl-ACP_6 and TE in *trans*

A [^{1}H, ^{15}N]-HSQC spectrum of butyryl-^{15}N-ACP_6 (1 mM) was recorded, TE_{S303A} (400 μM) was then added to the solution, and a second [^{1}H, ^{15}N]-HSQC spectrum was obtained. Similarly, [^{1}H, ^{15}N]-HSQC spectra were recorded of 2-methyl, 3-keto-diketide-^{15}N-ACP_6 and (2*RS*)-methylmalonate-^{15}N-ACP_6 (1 mM), and then TE (1 mM) was titrated in stepwise to give final ACP:TE ratios of 4:1, 2:1, and 1:1. For the positive control with Sfp, the PPTase was incubated with a 2-fold excess of CoA and Mg^{2+}. The Sfp (1 mM) was then titrated into a 1 mM sample of ACP (S2853A), to give final ACP:Sfp ratios of 4:1, 2:1, and 1:1.

ACCESSION NUMBERS

The chemical shift data for *apo* DEBS ACP_6 have been deposited with the BioMagResBank (BMRB) under accession number 16966.

SUPPLEMENTAL INFORMATION

Supplemental Information includes Supplemental Experimental Procedures and six figures and can be found online at doi:10.1016/j.chembiol.2010.05.017.

ACKNOWLEDGMENTS

We thank Peter Leadlay for his generous support of this research and for critical reading of this manuscript, Daniel Nietlispach for assistance with the NMR experiments, and Rinaldo Wander-Montalvao for facilitating the CHESHIRE calculations. We also acknowledge Bill Gerwick for suggesting the use of ^{13}C-butyrate, and Jim Staunton for helpful discussions. Funding for the initial stages of this work was provided by BBSRC project grant 8/B18119. L.T. also thanks Universities UK, the Cambridge Australia Trust, the Cambridge Commonwealth Trust, and Corpus Christi College for financial support.

Received: March 18, 2010
Revised: April 26, 2010
Accepted: May 3, 2010
Published: July 29, 2010

REFERENCES

Aggarwal, R., Caffrey, P., Leadlay, P.F., Smith, C.J., and Staunton, J. (1995). The thioesterase of the erythromycin-producing polyketide synthase–mechanistic studies *in vitro* to investigate its mode of action and substrate specificity. J. Chem. Soc. Chem. Commun., 1519–1520.

Akey, D.L., Kittendorf, J.D., Giraldes, J.W., Fecik, R.A., Sherman, D.H., and Smith, J.L. (2006). Structural basis for macrolactonization by the pikromycin thioesterase. Nat. Chem. Biol. *2*, 537–542.

Alekseyev, V.Y., Liu, C.W., Cane, D.E., Puglisi, J.D., and Khosla, C. (2007). Solution structure and proposed domain-domain recognition interface of an acyl carrier protein domain from a modular polyketide synthase. Protein Sci. *16*, 2093–2107.

Brignole, E.J., Smith, S., and Asturias, F.J. (2009). Conformational flexibility of metazoan fatty acid synthase enables catalysis. Nat. Struct. Mol. Biol. *16*, 190–197.

Bruner, S.D., Weber, T., Kohli, R.M., Schwarzer, D., Marahiel, M.A., Walsh, C.T., and Stubbs, M.T. (2002). Structural basis for the cyclization of the lipopeptide antibiotic surfactin by the thioesterase domain SrfTE. Structure *10*, 301–310.

Burfield, D.R., and Smithers, R.H. (1983). Desiccant efficiency in solvent and reagent drying. 7 Alcohols. J. Org. Chem. *48*, 2420–2422.

Cavalli, A., Salvatella, X., Dobson, C.M., and Vendruscolo, M. (2007). Protein structure determination from NMR chemical shifts. Proc. Natl. Acad. Sci. USA *104*, 9615–9620.

Chen, A.Y., Schnarr, N.A., Kim, C.Y., Cane, D.E., and Khosla, C. (2006). Extender unit and acyl carrier protein specificity of ketosynthase domains of the 6-deoxyerythronolide B synthase. J. Am. Chem. Soc. *128*, 3067–3074.

Chen, A.Y., Cane, D.E., and Khosla, C. (2007). Structure-based dissociation of a type I polyketide synthase module. Chem. Biol. *14*, 784–792.

Cortés, J., Wiesmann, K.E.H., Roberts, G.A., Brown, M.J.B., Staunton, J., and Leadlay, P.F. (1995). Repositioning of a domain in a modular polyketide synthase to promote specific chain cleavage. Science *268*, 1487–1489.

Evans, S.E., Williams, C., Arthur, C.J., Burston, S.G., Simpson, T.J., Crosby, J., and Crump, M.P. (2008). An ACP structural switch: conformational differences between the *apo* and *holo* forms of the actinorhodin polyketide synthase acyl carrier protein. Chembiochem *9*, 2424–2432.

Evans, S.E., Williams, C., Arthur, C.J., Ploskon, E., Wattana-Amorn, P., Cox, R.J., Willis, C.L., Crosby, J., Simpson, T.J., and Crump, M.P. (2009). Probing the interactions of early polyketide intermediates with the actinorhodin ACP from *S. coelicolor* A3(2). J. Mol. Biol. *389*, 511–528.

Findlow, S.C., Winsor, C., Simpson, T.J., Crosby, J., and Crump, M.P. (2003). Solution structure and dynamics of oxytetracycline polyketide synthase acyl carrier protein from *Streptomyces rimosus*. Biochemistry *42*, 8423–8433.

Fischbach, M.A., and Walsh, C.T. (2006). Assembly-line enzymology for polyketide and nonribosomal peptide antibiotics: logic, machinery, and mechanisms. Chem. Rev. *106*, 3468–3496.

Frueh, D.P., Arthanari, H., Koglin, A., Vosburg, D.A., Bennett, A.E., Walsh, C.T., and Wagner, G. (2008). Dynamic thiolation-thioesterase structure of a nonribosomal peptide synthetase. Nature *454*, 903–906.

Giraldes, J.W., Akey, D.L., Kittendorf, J.D., Sherman, D.H., Smith, J.L., and Fecik, R.A. (2006). Structural and mechanistic insights into polyketide macrolactonization from polyketide-based affinity labels. Nat. Chem. Biol. *2*, 531–536.

Hans, M., Hornung, A., Dziarnowski, A., Cane, D.E., and Khosla, C. (2003). Mechanistic analysis of acyl transferase domain exchange in polyketide synthase modules. J. Am. Chem. Soc. *125*, 5366–5374.

Hong, H., Leadlay, P.F., and Staunton, J. (2009). The changing patterns of covalent active site occupancy during catalysis on a modular polyketide synthase multienzyme revealed by ion-trap mass spectrometry. FEBS J. *276*, 7057–7069.

Jenke-Kodama, H., Börner, T., and Dittmann, E. (2006). Natural biocombinatorics in the polyketide synthase genes of the actinobacterium *Streptomyces avermitilis*. Plos Comp. Biol. *2*, e132.

Kapur, S., and Khosla, C. (2008). Biochemistry–fit for an enzyme. Nature *454*, 832–833.

Kim, C.Y., Alekseyev, V.Y., Chen, A.Y., Tang, Y., Cane, D.E., and Khosla, C. (2004). Reconstituting modular activity from separated domains of 6-deoxyerythronolide B synthase. Biochemistry *43*, 13892–13898.

Kim, Y., Kovrigin, E.L., and Eletr, Z. (2006). NMR studies of *Escherichia coli* acyl carrier protein: dynamic and structural differences of the *apo*- and *holo*-forms. Biochem. Biophys. Res. Commun. *341*, 776–783.

Koglin, A., Mofid, M.R., Lohr, F., Schafer, B., Rogov, V.V., Blum, M.M., Mittag, T., Marahiel, M.A., Bernhard, F., and Dotsch, V. (2006). Conformational

switches modulate protein interactions in peptide antibiotic synthetases. Science *312*, 273–276.

Lai, J.R., Koglin, A., and Walsh, C.T. (2006). Carrier protein structure and recognition in polyketide and nonribosomal peptide biosynthesis. Biochemistry *45*, 14869–14879.

Lambalot, R.H., Gehring, A.M., Flugel, R.S., Zuber, P., LaCelle, M., Marahiel, M.A., Reid, R., Khosla, C., and Walsh, C.T. (1996). A new enzyme superfamily–the phosphopantetheinyl transferases. Chem. Biol. *3*, 923–936.

Li, Q., Khosla, C., Puglisi, J.D., and Liu, C.W. (2003). Solution structure and backbone dynamics of the *holo* form of the frenolicin acyl carrier protein. Biochemistry *42*, 4648–4657.

Marsden, A.F., Caffrey, P., Aparicio, J.F., Loughran, M.S., Staunton, J., and Leadlay, P.F. (1994). Stereospecific acyl transfers on the erythromycin-producing polyketide synthase. Science *263*, 378–380.

Martin, C.J., Timoney, M.C., Sheridan, R.M., Kendrew, S.G., Wilkinson, B., Staunton, J., and Leadlay, P.F. (2003). Heterologous expression in *Saccharopolyspora erythraea* of a pentaketide synthase derived from the spinosyn polyketide synthase. Org. Biomol. Chem. *1*, 4144–4147.

Mayo, K.H., and Prestegard, J.H. (1985). Acyl carrier protein from *Escherichia coli*. Structural characterization of short-chain acylated acyl carrier proteins by NMR. Biochemistry *24*, 7834–7838.

Nazi, I., Koteva, K.P., and Wright, G.D. (2004). One-pot chemoenzymatic preparation of coenzyme A analogues. Anal. Biochem. *324*, 100–105.

Palmer, A.G., Cavanagh, J., Rance, M., Skelton, N.J., and Fairbrother, W.J. (2006). Protein NMR Spectroscopy: Principles and Practice, Second Edition (London: Academic Press Ltd.).

Ploskon, E., Arthur, C.J., Evans, S.E., Williams, C., Crosby, J., Simpson, T.J., and Crump, M.P. (2008). A mammalian type I fatty acid synthase acyl carrier protein domain does not sequester acyl chains. J. Biol. Chem. *283*, 518–528.

Quadri, L.E., Weinreb, P.H., Lei, M., Nakano, M.M., Zuber, P., and Walsh, C.T. (1998). Characterization of Sfp, a *Bacillus subtilis* phosphopantetheinyl transferase for peptidyl carrier protein domains in peptide synthetases. Biochemistry *37*, 1585–1595.

Roujeinikova, A., Baldock, C., Simon, W.J., Gilroy, J., Baker, P.J., Stuitje, A.R., Rice, D.W., Slabas, A.R., and Rafferty, J.B. (2002). X-ray crystallographic studies on butyryl-ACP reveal flexibility of the structure around a putative acyl chain binding site. Structure *10*, 825–835.

Roujeinikova, A., Simon, W.J., Gilroy, J., Rice, D.W., Rafferty, J.B., and Slabas, A.R. (2007). Structural studies of fatty acyl-(acyl carrier protein) thioesters reveal a hydrophobic binding cavity that can expand to fit longer substrates. J. Mol. Biol. *365*, 135–145.

Sambrook, J., and Russell, D.W. (2001). Molecular Cloning: A Laboratory Manual (Cold Spring Harbor, NY: Cold Spring Harbor Laboratory Press).

Samel, S.A., Schoenafinger, G., Knappe, T.A., Marahiel, M.A., and Essen, L.O. (2007). Structural and functional insights into a peptide bond-forming bidomain from a nonribosomal peptide synthetase. Structure *15*, 781–792.

Schwarzer, D., Mootz, H.D., Linne, U., and Marahiel, M.A. (2002). Regeneration of misprimed nonribosomal peptide synthetases by type II thioesterases. Proc. Natl. Acad. Sci. USA *99*, 14083–14088.

Smith, S., and Tsai, S.C. (2007). The type I fatty acid and polyketide synthases: a tale of two megasynthases. Nat. Prod. Rep. *24*, 1041–1072.

Staunton, J., and Weissman, K.J. (2001). Polyketide biosynthesis: a millennium review. Nat. Prod. Rep. *18*, 380–416.

Tang, Y., Kim, C.Y., Mathews, I.I., Cane, D.E., and Khosla, C. (2006). The 2.7-Å crystal structure of a 194-kDa homodimeric fragment of the 6-deoxyerythronolide B synthase. Proc. Natl. Acad. Sci. USA *103*, 11124–11129.

Tanovic, A., Samel, S.A., Essen, L.O., and Marahiel, M.A. (2008). Crystal structure of the termination module of a nonribosomal peptide synthetase. Science *321*, 659–663.

Tosin, M., Spiteller, D., and Spencer, J.B. (2009). Malonyl carba(dethia)- and malonyl oxa(dethia)-coenzyme A as tools for trapping polyketide intermediates. Chembiochem *10*, 1714–1723.

Tosin, M., Betancor, L., Stephens, E., Li, W.M., Spencer, J.B., and Leadlay, P.F. (2010). Synthetic chain terminators off-load intermediates from a type I polyketide synthase. Chembiochem *11*, 539–546.

Tran, L., Tosin, M., Spencer, J.B., Leadlay, P.F., and Weissman, K.J. (2008). Covalent linkage mediates communication between ACP and TE domains in modular polyketide synthases. Chembiochem *9*, 905–915.

Tsai, S.C., Miercke, L.J., Krucinski, J., Gokhale, R., Chen, J.C., Foster, P.G., Cane, D.E., Khosla, C., and Stroud, R.M. (2001). Crystal structure of the macrocycle-forming thioesterase domain of the erythromycin polyketide synthase: versatility from a unique substrate channel. Proc. Natl. Acad. Sci. USA *98*, 14808–14813.

Tsai, S.C., Lu, H.X., Cane, D.E., Khosla, C., and Stroud, R.M. (2002). Insights into channel architecture and substrate specificity from crystal structures of two macrocycle-forming thioesterases of modular polyketide synthases. Biochemistry *41*, 12598–12606.

Valenzano, C.R., Lawson, R.J., Chen, A.Y., Khosla, C., and Cane, D.E. (2009). The biochemical basis for stereochemical control in polyketide biosynthesis. J. Am. Chem. Soc. *131*, 18501–18511.

Wang, M., and Boddy, C.N. (2008). Examining the role of hydrogen bonding interactions in the substrate specificity for the loading step of polyketide synthase thioesterase domains. Biochemistry *47*, 11793–11803.

Wattana-Amorn, P., Williams, C., Ploskon, E., Cox, R.J., Simpson, T.J., Crosby, J., and Crump, M.P. (2010). Solution structure of an acyl carrier protein domain from a fungal type I polyketide synthase. Biochemistry *49*, 2186–2193.

Weber, T., Baumgartner, R., Renner, C., Marahiel, M.A., and Holak, T.A. (2000). Solution structure of PCP, a prototype for the peptidyl carrier domains of modular peptide synthetases. Structure *8*, 407–418.

Weissman, K.J. (2008). Taking a closer look at fatty acid biosynthesis. Chembiochem *9*, 2929–2931.

Weissman, K.J., and Leadlay, P.F. (2005). Combinatorial biosynthesis of reduced polyketides. Nat. Rev. Microbiol. *3*, 925–936.

Weissman, K.J., and Müller, R. (2008). Protein-protein interactions in multienzyme megasynthetases. Chembiochem *9*, 826–848.

Weissman, K.J., Hong, H., Oliynyk, M., Siskos, A.P., and Leadlay, P.F. (2004). Identification of a phosphopantetheinyl transferase for erythromycin biosynthesis in *Saccharopolyspora erythraea*. Chembiochem *5*, 116–125.

Weissman, K.J., Hong, H., Popovic, B., and Meersman, F. (2006). Evidence for a protein-protein interaction motif on an acyl carrier protein domain from a modular polyketide synthase. Chem. Biol. *13*, 625–636.

Wong, F.T., Chen, A.Y., Cane, D.E., and Khosla, C. (2010). Protein-protein recognition between acyltransferases and acyl carrier proteins in multimodular polyketide synthases. Biochemistry *49*, 95–102.

Wong, H.C., Liu, G., Zhang, Y.M., Rock, C.O., and Zheng, J. (2002). The solution structure of acyl carrier protein from *Mycobacterium tuberculosis*. J. Biol. Chem. *277*, 15874–15880.

Wu, B.N., Zhang, Y.M., Rock, C.O., and Zheng, J.J. (2009). Structural modification of acyl carrier protein by butyryl group. Protein Sci. *18*, 240–246.

Xu, G.Y., Tam, A., Lin, L., Hixon, J., Fritz, C.C., and Powers, R. (2001). Solution structure of *B. subtilis* acyl carrier protein. Structure *9*, 277–287.

Yeh, E., Kohli, R.M., Bruner, S.D., and Walsh, C.T. (2004). Type II thioesterase restores activity of a NRPS module stalled with an aminoacyl-*S*-enzyme that cannot be elongated. Chembiochem *5*, 1290–1293.

Zhang, Y. (2009). I-TASSER: fully automated protein structure prediction in CASP8. Proteins *77* (*Suppl. 9*), 100–113.

Zornetzer, G.A., Fox, B.G., and Markley, J.L. (2006). Solution structures of spinach acyl carrier protein with decanoate and stearate. Biochemistry *45*, 5217–5227.

